



ELSEVIER

10 September 1999

Chemical Physics Letters 310 (1999) 471–476

**CHEMICAL
PHYSICS
LETTERS**

www.elsevier.nl/locate/cplett

Observation of the $y^1\Pi_g-c'_4{}^1\Sigma_u^+$ and $k^1\Pi_g-c'_4{}^1\Sigma_u^+$ systems of N_2

Arno de Lange *, Wim Ubachs

Department of Physics and Astronomy, Vrije Universiteit, De Boelelaan 1081, 1081 HV Amsterdam, The Netherlands

Received 25 June 1999

Abstract

We observed the Λ -doublet of both parity components of the (1,0) band of the $y^1\Pi_g-c'_4{}^1\Sigma_u^+$ and $k^1\Pi_g-c'_4{}^1\Sigma_u^+$ systems of molecular nitrogen in an extreme ultraviolet (XUV) + infrared (IR) double resonance experiment. The (e) components as well as the (f) components are observed up to $J=21$ in the case of the y state and up to $J=17$ in the case of the k state. Apart from mutual interaction between $y^1\Pi_g$ and $k^1\Pi_g$, the (e) components undergo additional perturbations giving rise to predissociation. © 1999 Elsevier Science B.V. All rights reserved.

1. Introduction

The $y^1\Pi_g$ state is the upper state in Kaplan's first ($y^1\Pi_g-d'{}^1\Sigma_u^-$) and second ($y^1\Pi_g-w{}^1\Delta_u$) systems in N_2 . Though the first observation of the second system was by Duncan in 1925 [1], it was Kaplan who recognized the structure in the series [2–4]. Lofthus and Mulliken [5] remeasured and added several bands to Kaplan's first and second systems and assigned $^1\Pi_g$ symmetry to the y state. The low intensity of the lines involving (e) components of y ($v=0$) and the total absence of the (e) components of y ($v=1$) in emission was ascribed to predissociation. An interaction with a $^1\Sigma_g^+$ state was proposed as the predissociation mechanism, since any other singlet *gerade* species would also affect the levels of the (f) component.

The $k^1\Pi_g$ state is the upper state in Carroll–Subbaram I ($k^1\Pi_g-d'{}^1\Sigma_u^-$) and II ($k^1\Pi_g-w{}^1\Delta_u$) systems, observed for the first time in 1975 [6]. The y ($v=0,1,2$) states were also observed and it was found that the $y^1\Pi_g$ and $k^1\Pi_g$ states exhibit a very strong mutual homogeneous interaction, which explains the strong perturbation in the rotational structure, especially for the $v=1$ vibrational level, as was previously observed in the y state by Lofthus and Mulliken [5]. In the case of the k state a similar predissociation process was observed as in the case of the y state; low intensities for the (e) components of $v=0$ and a total absence of the (e) components of $v=1$. An indirect predissociation mechanism was postulated involving the lowest excited $^1\Sigma_g^+$ state converging to the dissociation limit ${}^2D+{}^2D$ and the dissociation continuum of the ${}^3\Sigma_g^-$ state correlating with ${}^4S+{}^2P$.

Whereas the experiments mentioned above involved emission spectroscopy, multi-step laser excitation is used in the present Letter. The (1,0) band of the $y-c'_4$ and $k-c'_4$ systems have been observed in

* Corresponding author. Fax: +1-31-20-444-7999; e-mail: arno@nat.vu.nl

the near infrared ($\lambda \approx 867$ nm), with the $c'_4 \ ^1\Sigma_u^+$ state used as intermediate. Both parity components of the $v = 1$ vibrational level of the y and k states are observed and further evidence is found for the indirect predissociation process suggested by Carroll and Subbaram [6].

2. Experiment

The $y \ ^1\Pi_g$ ($v = 1$) and the $k \ ^1\Pi_g$ ($v = 1$) states are investigated in a extreme ultraviolet (XUV) + infrared (IR) double resonance scheme, with the $c'_4 \ ^1\Sigma_u^+$ ($v = 0$) state as an intermediate. The excitation scheme as well as the potential curves of relevance for the present Letter are depicted in Fig. 1. The general features of the apparatus are similar to the one used for the investigation of double resonance spectra in molecular hydrogen [7]. Wave-

length-tunable XUV radiation around 96 nm is used to drive the transition from the $X \ ^1\Sigma_g^+$ electronic ground state to a rotationally selected level of the lowest Rydberg state in nitrogen, the $c'_4 \ ^1\Sigma_u^+$ ($v = 0$) state. To induce transitions from the $c'_4 \ ^1\Sigma_u^+$ state to the $y \ ^1\Pi_g$ and $k \ ^1\Pi_g$ states, a second laser, tunable in the infrared near 867 nm, is used. The pulses of the XUV and IR lasers, each of 3–5 ns duration, are temporally overlapped in the interaction region in view of the short lifetime (< 1 ns) of the $c'_4 \ ^1\Sigma_u^+$ intermediate state [8]. A third laser at $\lambda = 532$ nm is used to ionize N_2 from the y or k state, and hence the detection of N_2^+ ions can be used to record the double resonance spectra, in this case of the $y \ ^1\Pi_g - c'_4 \ ^1\Sigma_u^+$ (1,0) and $k \ ^1\Pi_g - c'_4 \ ^1\Sigma_u^+$ (1,0) bands. For further details on the generation of tunable XUV radiation and its application to the spectroscopy of N_2 we refer to Ref. [9].

The level energies of the c'_4 state are known with an accuracy of ~ 0.03 cm^{-1} [10] and therefore only the radiation from the second dye laser needs to be wavelength calibrated to obtain level energies of $y \ ^1\Pi_g$ ($v = 1$) and $k \ ^1\Pi_g$ ($v = 1$) rotational states with respect to the $X \ ^1\Sigma_g^+$ ($v = 0, J = 0$) ground state. Since no standard reference is available around 867 nm, the infrared light was frequency-doubled to record a Te_2 -absorption spectrum (510°C) simultaneously with the double resonance spectra of N_2 . Through fitting of the Te_2 resonances with Gaussian profiles and assigning the peak positions with the Te_2 atlas [11], an accurate frequency scale was constructed for the infrared. At low intensities of the infrared radiation, the linewidth of the N_2 absorption lines was ~ 0.08 cm^{-1} , equal to the laser linewidth of the second laser.

The effects of predissociation in laser excitation experiments can in principle be observed through line broadening. However, if the bandwidth of the lasers exceeds the Fourier-transform limit, as in the present Letter, even predissociation yields of up to 99% cannot be observed via line broadening. The present three-laser configuration provides two methods to derive quantitative information on the excited state lifetimes and predissociation rates. First, pulses from the third laser, used to ionize the $y \ ^1\Pi_g$ and $k \ ^1\Pi_g$ excited state population, can be subject to a variable delay. From this procedure we deduce that the lifetime of the (f) components of both $y \ ^1\Pi_g$

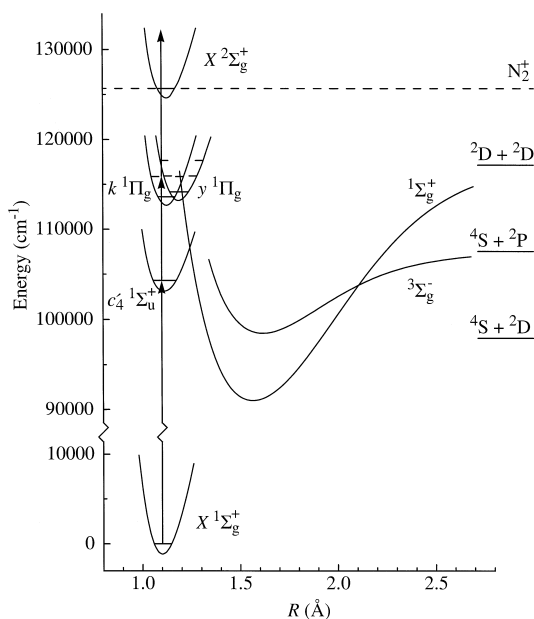


Fig. 1. Excitation scheme and potential energy curves for N_2 . The transition $c'_4 \ ^1\Sigma_u^+ - X \ ^1\Sigma_g^+$ is induced by a XUV laser and the transitions $y \ ^1\Pi_g - c'_4 \ ^1\Sigma_u^+$ and $k \ ^1\Pi_g - c'_4 \ ^1\Sigma_u^+$ are driven by a temporally overlapped IR laser. A third laser at 532 nm is used to ionize molecular nitrogen from the y and k excited states. The curve of the $^1\Sigma_g^+$ state is based on ab initio calculations from Dateo [16], whereas the curve of the $^3\Sigma_g^-$ is based on ab initio calculations from Partridge [17].

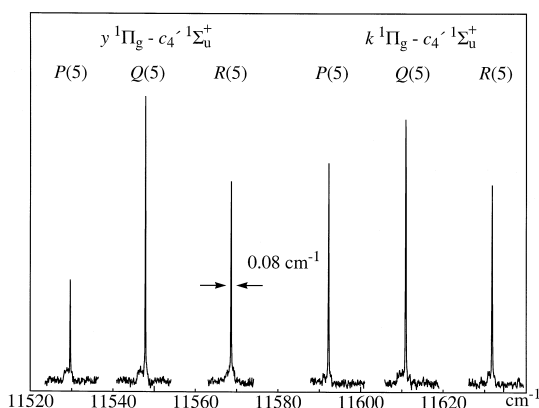


Fig. 2. A double resonance spectrum with the $c'_4^1\Sigma_u^+$ ($v=0, J=5$) as the intermediate state. The intensity of the second laser is reduced to avoid saturation broadening; the linewidth equals the laser bandwidth ($\sim 0.08 \text{ cm}^{-1}$).

and $k^1\Pi_g$ is about 20 ns, in agreement with the value found by Hummer and Burns [12]. For signal recording in excitation via the (e) components the third laser had to be temporally overlapped, demon-

strating that the (e) components are shorter lived. As previously explained in more detail [13] the line intensities in resonance enhanced multi-step excitation decrease if predissociation becomes a competitive process. Indeed for the higher J levels of the (e) component of both $y^1\Pi_g$ ($v=1$) and $k^1\Pi_g$ ($v=1$) states, such intensity decrease, even to the extent of missing lines, is observed.

3. Results and discussion

In Fig. 2 a typical double resonance spectrum is depicted for the $c'_4^1\Sigma_u^+$ ($v=0, J=5$) intermediate state. In the case of electric dipole transitions, up to three transitions within one band can be observed in such a spectrum, each corresponding to one of the P , Q and R branches. Double resonance spectra have two advantages over single photon spectra; blending of lines will be avoided in most cases and the identification of the upper level is less complex as

Table 1

Observed line positions in the $y^1\Pi_g-c'_4^1\Sigma_u^+$ and $k^1\Pi_g-c'_4^1\Sigma_u^+$ systems. Values in cm^{-1} . The estimated uncertainty in the transition frequencies is 0.03 cm^{-1} .

| J | $y^1\Pi_g-c'_4^1\Sigma_u^+$ (1,0) | | | $k^1\Pi_g-c'_4^1\Sigma_u^+$ (1,0) | | |
|-----|-----------------------------------|----------|----------|-----------------------------------|----------|----------|
| | $P(J)$ | $Q(J)$ | $R(J)$ | $P(J)$ | $Q(J)$ | $R(J)$ |
| 0 | – | – | 11555.12 | – | – | 11617.81 |
| 1 | – | – | 11558.48 | – | – | 11621.17 |
| 2 | 11543.60 | 11550.75 | 11561.53 | 11606.28 | 11613.56 | 11624.21 |
| 3 | 11539.19 | 11550.08 | 11564.32 | 11601.85 | 11612.93 | 11626.96 |
| 4 | 11534.62 | 11549.08 | 11566.67 | 11597.22 | 11612.00 | 11629.58 |
| 5 | 11529.65 | 11547.88 | 11568.70 | 11592.26 | 11610.97 | 11631.81 |
| 6 | 11524.38 | 11546.44 | 11570.36 | 11587.25 | 11609.79 | – |
| 7 | 11518.82 | 11544.64 | 11571.59 | 11582.03 | 11608.57 | 11636.09 |
| 8 | 11512.93 | 11542.81 | 11572.43 | 11576.65 | 11607.34 | 11638.00 |
| 9 | 11506.82 | 11540.79 | 11572.78 | 11571.26 | 11606.20 | 11639.86 |
| 10 | 11501.08 | 11539.21 | 11573.57 | 11566.65 | 11605.90 | 11641.41 |
| 11 | 11488.99 | 11531.52 | – | – | 11599.80 | – |
| 12 | 11482.63 | 11529.87 | – | – | 11600.09 | – |
| 13 | 11474.21 | 11526.54 | – | 11548.67 | 11599.27 | 11646.94 |
| 14 | – | 11522.70 | 11573.65 | 11542.60 | 11598.44 | 11649.12 |
| 15 | – | 11518.49 | 11568.86 | 11537.11 | 11597.68 | – |
| 16 | 11456.47 | 11513.95 | 11564.71 | 11531.92 | 11597.12 | – |
| 17 | 11444.36 | 11509.05 | 11559.92 | – | 11596.85 | 11657.26 |
| 18 | – | 11504.04 | 11552.59 | 11522.10 | – | – |
| 19 | – | 11498.82 | – | – | – | – |
| 20 | – | 11493.55 | – | – | – | – |
| 21 | 11415.28 | 11488.18 | – | – | – | – |

the total angular momentum J may differ up to one, with respect to the known intermediate state. The observed lines of the $y^1\Pi_g-c_4^1\Sigma_u^+$ (1,0) and $k^1\Pi_g-c_4^1\Sigma_u^+$ (1,0) bands are listed in Table 1. The level energies of both states, with respect to the $X^1\Sigma_g^+$ ($v=0, J=0$) ground state, are obtained by adding the infrared transition frequencies to the calculated level energies of the rotational states of $c_4^1\Sigma_u^+$ ($v=0$). Level energies up to $J=19$ can be computed from the molecular constants with deviations between observed and calculated energies of $\sim 0.04 \text{ cm}^{-1}$ when the mutual homogeneous interaction with the $b^1\Sigma_u^+$ ($v=1$) state is taken into account [10]. Since this model for the level structure of $c_4^1\Sigma_u^+$ ($v=0$) breaks down for $J > 19$ the observed values are used for $J=20$ and $J=21$ [10]. The resulting level energies for the $y^1\Pi_g$ ($v=1$) and $k^1\Pi_g$ ($v=1$) states are listed in Table 2.

As discussed by Carroll and Subbaram [6] the $y^1\Pi_g$ and the $k^1\Pi_g$ states undergo a strong mutual homogeneous interaction. The energy levels of both

the y and k states are fitted simultaneously to eigenvalues of the matrix

$$\begin{pmatrix} E_y & H_{yk} \\ H_{yk} & E_k \end{pmatrix}, \quad (1)$$

where H_{yk} represents the J -independent matrix element for a homogeneous interaction between the y and k states, and E_y and E_k represent the deperturbed energy levels of the y and k states respectively, given by the formulae:

$$E_y = \nu_{10,y} + B_y [J(J+1) - \Lambda^2] - D_y [J(J+1) - \Lambda^2]^2, \quad (2)$$

$$E_k = \nu_{10,k} + B_k [J(J+1) - \Lambda^2] - D_k [J(J+1) - \Lambda^2]^2, \quad (3)$$

where ν_{10} represents the band origin, B the rotational constant and D a centrifugal distortion parameter. The values for D_y and D_k are kept fixed at calculated values. If for the potential function a

Table 2

The obtained level energies of the (e) and (f) components of the $y^1\Pi_g$ ($v=1$) and $k^1\Pi_g$ ($v=1$) states, with respect to the $X^1\Sigma_g^+$ ($v=0, J=0$) ground state. Deviations between experimentally determined energies and the ones calculated from the molecular constants given in Table 3 are given in the columns under Δ_{oc} . All values in cm^{-1} . The estimated uncertainty in the level energies is 0.04 cm^{-1} .

| J | $y^1\Pi_g$ (e) | | $y^1\Pi_g$ (f) | | $k^1\Pi_g$ (e) | | $k^1\Pi_g$ (f) | |
|-----|--------------------|---------------|--------------------|---------------|--------------------|---------------|--------------------|---------------|
| | energy | Δ_{oc} | energy | Δ_{oc} | energy | Δ_{oc} | energy | Δ_{oc} |
| 1 | 115877.79 | 0.09 | – | – | 115940.47 | –0.03 | – | – |
| 2 | 115884.98 | 0.12 | 115884.97 | –0.02 | 115947.65 | –0.02 | 115947.77 | –0.03 |
| 3 | 115895.78 | 0.20 | 115895.86 | 0.02 | 115958.41 | –0.02 | 115958.71 | 0.01 |
| 4 | 115910.10 | 0.24 | 115910.26 | –0.03 | 115972.71 | –0.09 | 115973.19 | –0.05 |
| 5 | 115927.86 | 0.19 | 115928.31 | –0.02 | 115990.75 | –0.04 | 115991.40 | –0.05 |
| 6 | 115949.13 | 0.12 | 115949.92 | –0.01 | 116012.30 | –0.11 | 116013.28 | –0.06 |
| 7 | 115973.84 | –0.01 | 115975.06 | –0.01 | 116037.56 | –0.12 | 116038.89 | –0.03 |
| 8 | 116001.92 | –0.24 | 116003.72 | –0.01 | 116066.40 | –0.24 | 116068.26 | 0.02 |
| 9 | 116033.34 | –0.59 | 116035.90 | 0.02 | 116098.84 | –0.39 | 116101.31 | 0.01 |
| 10 | 116067.97 | –1.14 | 116071.46 | –0.03 | 116134.97 | –0.71 | 116138.16 | 0.02 |
| 11 | 116105.82 | –1.86 | 116110.57 | 0.04 | 116173.67 | –2.15 | 116178.85 | 0.08 |
| 12 | 116146.49 | –3.13 | 116153.06 | 0.08 | 116220.95 | 1.22 | 116223.28 | 0.05 |
| 13 | – | – | 116198.82 | 0.01 | 116267.89 | 0.45 | 116271.55 | 0.02 |
| 14 | – | – | 116247.99 | –0.01 | 116319.19 | 0.23 | 116323.73 | 0.04 |
| 15 | 116298.93 | 3.53 | 116300.52 | –0.01 | 116374.39 | 0.09 | 116379.72 | –0.01 |
| 16 | 116350.86 | 0.27 | 116356.39 | –0.01 | – | – | 116439.57 | –0.07 |
| 17 | 116407.15 | –1.92 | 116415.52 | –0.07 | 116496.17 | –0.32 | 116503.32 | –0.11 |
| 18 | 116466.39 | –4.44 | 116478.11 | 0.01 | 116563.73 | 0.40 | – | – |
| 19 | 116526.66 | –9.21 | 116544.02 | 0.09 | – | – | – | – |
| 20 | 116612.54 | 8.36 | 116613.14 | 0.06 | – | – | – | – |
| 21 | – | – | 116685.43 | –0.11 | – | – | – | – |

power series around the equilibrium distance R_e is used, it can be shown [14] that

$$D_v = \left(\frac{4B_e^3}{\omega_e^2} \right) \left[1 + \left(\frac{8\omega_e x_e}{\omega_e} - \frac{5\alpha_e}{B_e} - \frac{\alpha_e^2 \omega_e}{24B_e^3} \right) \times \left(v + \frac{1}{2} \right) \right]. \quad (4)$$

With this formula and the constants taken from Ref. [6] D_y was determined to be $D_y = 6.7 \times 10^{-6} \text{ cm}^{-1}$. This procedure cannot be used to determine D_k , as only two vibrational levels, $v = 0$ and $v = 1$, have been observed up to now. Since the k state is a Rydberg state in a series converging towards the electronic groundstate of N_2^+ , D_k was kept fixed at $D_k = 6.6 \times 10^{-6} \text{ cm}^{-1}$, which is the value of the $\text{N}_2^+ X^2\Sigma_g^+$ ($v = 1$) state. Resulting parameters from a least-squares fitting procedure are tabulated in Table 3 while the deviations between observed and calculated levels are included in Table 2.

In Fig. 3 it can be seen that the levels of the (f) component (open markers) fit very well to the above formulae with $E_{\text{obs}} - E_{\text{calc}} \approx 0.04 \text{ cm}^{-1}$. The levels of the (e) component (filled markers), however, deviate strongly from the calculated values for both k (circles) and y (squares) states, such that no consistent analysis could be given on the basis of a two-state interaction model. The rotational B parameter derived for the (e) components is lower than for the (f) components and is represented here by a parameter q for the Λ -doubling as $B(e) = B(f) + q$. The ordering of the energy levels of the (f) component as a function of $J(J+1)$, as depicted in Fig. 3, shows anti-crossing patterns that are indicative of additional perturbations by bound states. In fact the q parameters as given in Table 3 for both k and y

Table 3

Molecular constants of the $y^1\Pi_g$ ($v = 1$) and $k^1\Pi_g$ ($v = 1$) states, as derived from a least squares fit. All values in cm^{-1} .

| | $y^1\Pi_g$ ($v = 1$) | $k^1\Pi_g$ ($v = 1$) |
|------------|-----------------------------------|-----------------------------------|
| ν_{10} | 115905.33(7) | 115905.71(8) |
| B | 1.7127(2) | 1.9122(3) |
| q | -0.021 ^a | -0.023 ^a |
| D | 6.7×10^{-6} ^a | 6.6×10^{-6} ^a |
| H_{y_k} | 31.40(2) | |

^a Estimated; kept fixed.

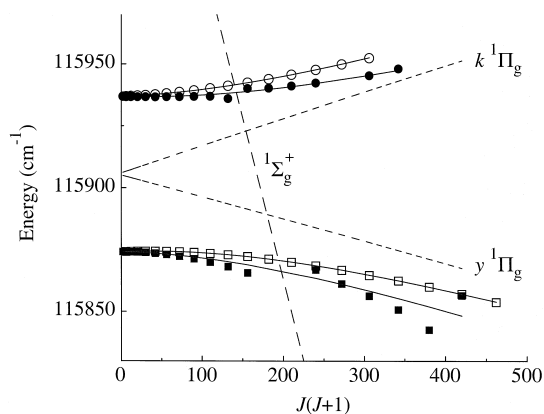


Fig. 3. Level energies plotted as a function of $J(J+1)$. For clarity $1.8 \times J(J+1)$ is subtracted from the level energies. The circles correspond to the $k^1\Pi_g$ ($v = 1$) state and the squares to the $y^1\Pi_g$ ($v = 1$) state. The (f) components are indicated with open markers and the (e) components with filled markers. The solid lines represent the fitted values with parameters given in Table 3 and the short-dashed lines correspond to the unperturbed energy levels of the (f) components. Also, the predissociated perturber is tentatively drawn (long-dashed).

states are set at values such that the anti-crossing patterns appear symmetric.

In both the $y^1\Pi_g - c_4^1\Sigma_u^+$ (1,0) and $k^1\Pi_g - c_4^1\Sigma_u^+$ (1,0) bands, the intensities of the P and R lines, representing the transitions to the (e) component, decrease much faster with increasing J , compared to the Q transitions probing the (f) component. In a REMPI experiment this is an indication of predissociation [9]. The intensities reach a minimum around the avoided crossings and in the case of the $y^1\Pi_g$ state $J = 13$ and $J = 14$ are missing. Beyond the avoided crossings the intensities of the (e) components tend to grow again towards the same signal strength as the (f) components. This strongly suggests that the perturbations in the energy levels are linked to predissociation.

Carroll and Subbaram [6] did not observe the (e) component of $v = 1$ and to explain this; it was suggested that this component was predissociated by a $^1\Sigma_g^+$ state. However, the lowest dissociation limit to which a $^1\Sigma_g^+$ state can converge, is $^2D + ^2D$ at 14.522 eV (besides the $^4S + ^4S$ at 9.756 eV, the dissociation limit of the $X^1\Sigma_g^+$ ground state), 0.151 eV above the k state. Therefore, an indirect predissociation mechanism was proposed, involving the low-

est excited $^1\Sigma_g^+$ state converging to the $^2D + ^2D$ dissociation limit and the $^3\Sigma_g^-$ state converging to the $^4S + ^2P$ dissociation limit (see also Fig. 1). As argued by Carroll and Subbaram [6] the $^3\Sigma_g^-$ causes predissociation in the $^1\Sigma_g^+$ state through an intersystem interaction. This $^1\Sigma_g^+$ state was first studied theoretically by Michels in 1970 [15] and it was found to be a valence state containing bound levels. Recently ab initio calculations were performed by Dateo [16] and the $^1\Sigma_g^+$ curve presented in Fig. 1 is derived from this Letter. The $y^1\Pi_g$ and $k^1\Pi_g$ states as well as the $^1\Sigma_g^+$ valence state have bound levels and therefore avoided crossings are to be expected. As can be seen in Fig. 3, avoided crossings seem to be present between $J = 11$ and $J = 12$ in the k state and between $J = 12$ and $J = 15$ in the y state. If the same state is responsible for both crossings, then the rotational B constant can be estimated graphically to be $B \sim 0.49 \text{ cm}^{-1}$. The perturber is tentatively drawn in the same figure. It is calculated, using the potential curves by Dateo [16], that the $^1\Sigma_g^+$ ($v \sim 35$) level falls in the energy region of the k and y states. The estimated value for the rotational constant of $B \sim 0.49 \text{ cm}^{-1}$ is in reasonable agreement with the calculated value of $B = 0.53 \text{ cm}^{-1}$ derived from the ab initio curve.

A second perturbation appears to be present at higher values of J for the (e) components of both y and k states. For the $y^1\Pi_g$ ($v = 1$) state large level shifts are observed near $J = 19$, while in the $k^1\Pi_g$ ($v = 1$) state a line is missing at $J = 16$, a clear indication of an accidental predissociation. The vibrational level spacing in the $^1\Sigma_g^+$ state, causing the perturbations at lower J , is calculated at 340 cm^{-1} near the excitation energy of k , y ($v = 1$) [16]. This value cannot be matched consistently with the energy separation between the two regions of interaction in the k and y states. Hence it is postulated that another state causes the perturbation effects at higher J .

4. Conclusion

The (1, 0) band of the $y^1\Pi_g - c'_4^1\Sigma_u^+$ and $k^1\Pi_g - c'_4^1\Sigma_u^+$ systems and the (e) components of $y^1\Pi_g$ ($v = 1$) and $k^1\Pi_g$ ($v = 1$) are observed for the first

time. The observed anti-crossings in the (e) component of the y and k states indicate that the perturbing state is a $^1\Sigma_g^+$ species, supporting bound levels. The behaviour of the line intensities around the anti-crossings proves that the level shifts are linked to predissociation. The suggestion, made by Carroll and Subbaram [6], that the (e) components of the $y^1\Pi_g$ ($v = 1$) and $k^1\Pi_g$ ($v = 1$) states are indirectly predissociated by a $^1\Sigma_g^+$ state, is verified. The present experimental Letter shows that excitation of *gerade* Rydberg states in molecular nitrogen is feasible in XUV + IR double resonance laser excitation. This method may in future be applied to uncover the entire manifold of highly excited *gerade* states in nitrogen.

Acknowledgements

The authors wish to thank H. Partridge and C. Dateo for making available results on an ab initio calculation prior to publication. They wish to acknowledge The Netherlands Foundation for Fundamental Research on Matter (FOM) for financial support.

References

- [1] D.C. Duncan, *Astrophys. J.* 62 (1925) 145.
- [2] J. Kaplan, *Phys. Rev.* 46 (1934) 534.
- [3] J. Kaplan, *Phys. Rev.* 46 (1934) 631.
- [4] J. Kaplan, *Phys. Rev.* 47 (1935) 259.
- [5] A. Lofthus, R.S. Mulliken, *J. Chem. Phys.* 26 (1957) 1010.
- [6] P.K. Carroll, K.V. Subbaram, *Can. J. Phys.* 53 (1975) 2198.
- [7] E. Reinhold, A. de Lange, W. Hogervorst, W. Ubachs, *J. Chem. Phys.* 109 (1998) 9772.
- [8] W. Ubachs, *Chem. Phys. Lett.* 268 (1997) 210.
- [9] W. Ubachs, K.S.E. Eikema, W. Hogervorst, *Appl. Phys. B* 57 (1993) 411.
- [10] P.F. Levelt, W. Ubachs, *Chem. Phys.* 163 (1992) 263.
- [11] J. Cariou, P. Luc, *Atlas du spectra d'absorption de la molécule de tellure*, Orsay, 1980.
- [12] C.R. Hummer, D.J. Burns, *J. Chem. Phys.* 67 (1977) 4062.
- [13] K.S.E. Eikema, W. Hogervorst, W. Ubachs, *Chem. Phys.* 181 (1994) 217.
- [14] G. Herzberg, *Spectra of Diatomic Molecules*, Grieger, Malabar, FL, 1991.
- [15] H.H. Michels, *J. Chem. Phys.* 53 (1970) 841.
- [16] C. Dateo, private communication.
- [17] H. Partridge, private communication.